



OPEN ACCESS

EDITED BY

Sergio G. Longhitano,
University of Basilicata, Italy

REVIEWED BY

Irene Cornacchia,
Italian National Research Council, Italy
Gregory Price,
University of Plymouth, United Kingdom

*CORRESPONDENCE

André Bornemann,
✉ andre.bornemann@bgr.de

RECEIVED 24 February 2023

ACCEPTED 26 May 2023

PUBLISHED 15 June 2023

CITATION

Bornemann A, Erbacher J, Blumenberg M and Voigt S (2023), A first high-resolution carbon isotope stratigraphy from the Boreal (NW Germany) for the Berriasian to Coniacian interval—implications for the timing of the Aptian–Albian boundary. *Front. Earth Sci.* 11:1173319. doi: 10.3389/feart.2023.1173319

COPYRIGHT

© 2023 Bornemann, Erbacher, Blumenberg and Voigt. This is an open-access article distributed under the terms of the [Creative Commons Attribution License \(CC BY\)](https://creativecommons.org/licenses/by/4.0/). The use, distribution or reproduction in other forums is permitted, provided the original author(s) and the copyright owner(s) are credited and that the original publication in this journal is cited, in accordance with accepted academic practice. No use, distribution or reproduction is permitted which does not comply with these terms.

A first high-resolution carbon isotope stratigraphy from the Boreal (NW Germany) for the Berriasian to Coniacian interval—implications for the timing of the Aptian–Albian boundary

André Bornemann^{1,2*}, Jochen Erbacher^{1,2}, Martin Blumenberg¹ and Silke Voigt³

¹Bundesanstalt für Geowissenschaften und Rohstoffe (BGR), Hannover, Germany, ²Landesamt für Bergbau, Energie und Geologie, Hannover, Germany, ³Goethe-Universität Frankfurt, Institut für Geowissenschaften, Frankfurt, Germany

High-amplitude changes in sedimentary $\delta^{13}\text{C}$ characterize the Cretaceous system and have been proven useful for supra-regional chemostratigraphic correlation. In the Cretaceous, these $\delta^{13}\text{C}$ perturbations indicate large shifts between the global carbon reservoirs that are usually caused by volcanic activity of large igneous provinces, the widespread deposition of thick organic carbon-rich sequences and/or changes in orbital parameters. Here, we present an upper Berriasian to lower Coniacian (c. 142–88 Ma) composite carbon isotope record based on 14 drill cores, 2 outcrops, and almost 5,000 samples. The total record comprises a composite thickness of more than 1,500 m. All cores and successions are located in the larger Hanover area, which represents the depocenter of the North German Lower Saxony Basin in Early to mid-Cretaceous times. In Northern Germany, Boreal Lower Cretaceous sediments are predominantly represented by CaCO_3 -poor mud and siltstones of up to 2,000 m thickness, which become more carbonate-rich during the Albian–Cenomanian transition and even chalkier in the upper Cenomanian to Coniacian interval. The carbon isotope record reveals a number of global key events, including the Valanginian Weissert Event, the Oceanic Anoxic Events (OAEs) 1a and d, and the Kilian Event (Aptian–Albian boundary, part of OAE 1b). For the early Late Cretaceous, the Mid-Cenomanian Event, the OAE 2 (Cenomanian–Turonian Boundary Event), and the Navigation Event, among others, have been identified. The Kilian Event represents the Aptian–Albian boundary and has been identified herein for the first time in Northern Europe. Based on the evaluation of its relative position to the Vöhrum boundary tuff, we tentatively propose a slightly older age for the Aptian–Albian boundary of c. 113.65 Ma instead of 113.2 Ma. The observed chemostratigraphic events enable a detailed stratigraphic comparison with Tethyan and other Boreal records and associated paleoenvironmental data. Thus, this new detailed chemostratigraphy provides a unique opportunity to potentially overcome many still existing Boreal–Tethyan correlation issues. The presented record can be considered almost complete, albeit a 2-Myr gap during the early Albian is likely, and condensed intervals occur specifically during the lower Aptian.

KEYWORDS

Cretaceous, carbon isotope ($\delta^{13}\text{C}$), stratigraphy, Northern Germany, Aptian-Albian boundary

1 Introduction

Chemostratigraphy has been proven to detect synchronous changes in element abundances and/or isotope ratios that can be used for stratigraphic correlation. Specifically, stable carbon isotopes ($\delta^{13}\text{C}$) of carbonates and oxygen isotopes of foraminiferal tests are powerful tools allowing for high-resolution chemostratigraphy in the Cenozoic (e.g., Maslin and Swann, 2006; Cramer et al., 2009; Westerhold et al., 2020) and the Mesozoic (e.g., Martinez et al., 2015; Batenburg et al., 2018) down to orbital time scales or even beyond. Nearly half a century ago, systematic changes in the $\delta^{13}\text{C}$ composition of Cretaceous marine carbonates ($\delta^{13}\text{C}_{\text{carb}}$) were documented for the first time (e.g., Weissert, 1979; Scholle and Arthur, 1980). In the subsequent years and decades, the temporal resolution of these records increased continuously (e.g., Renard, 1986; Schlanger et al., 1987; Lini et al., 1992; Jenkyns et al., 1994; Erbacher et al., 1996; Herrle et al., 2004; Jarvis et al., 2006; Voigt et al., 2008; Kim et al., 2022). Our understanding of the underlying mechanisms in the Earth system and the global carbon cycle driving these contemporaneous, globally observed swings in $\delta^{13}\text{C}$ at various timescales has been significantly improved based on such high-resolution datasets.

Carbon isotope-based chemostratigraphy is considered the most reliable method in pelagic carbonates. Major fluctuations in $\delta^{13}\text{C}$ have also been documented in shallow marine successions, organic carbon, and terrestrial settings (e.g., Wortmann and Weissert, 2000; Erbacher et al., 2005; Gröcke et al., 2005; Weissert et al., 2008; Huck et al., 2011), allowing land–sea correlations and, thus, reflecting global shifts between Earth's carbon pools. Specifically, $\delta^{13}\text{C}$ measurements on organic matter ($\delta^{13}\text{C}_{\text{org}}$) were successfully applied to high-resolution chemostratigraphy in organic-rich, carbonate-poor marine Cretaceous sediments (e.g., Menegatti et al., 1998; Erbacher et al., 2005).

The mid-Cretaceous period (~125–80 Ma) witnessed a number of widespread black shale occurrences that are named Oceanic Anoxic Events (OAEs). These OAEs are associated with dramatic changes in climate and biota (e.g., Erbacher et al., 1996; Leckie et al., 2002; Erba, 2006). These OAEs are attributed to intermittent global carbon cycle perturbations in the ocean–atmosphere system (e.g., Jarvis et al., 2006; Jenkyns, 2010). The influx of huge amounts of greenhouse gases such as CO_2 and/or CH_4 of predominantly volcanic origin has been considered the most important reason for global warming and oceanic anoxia. In turn, the widespread marine deposition of organic carbon during the OAEs, together with intensified chemical weathering, has been linked to the drawdown of atmospheric $p\text{CO}_2$ and global cooling (McAnena et al., 2013; Jenkyns, 2018; von Strandmann et al., 2020) and left their imprint in the global carbon cycle as reflected by $\delta^{13}\text{C}$. Potential causes for Cretaceous $\delta^{13}\text{C}$ anomalies associated with widespread black shale deposits are summarized by Jenkyns et al. (1994). On the contrary, carbon isotope events such as the Valanginian Weissert Event and the Hauterivian Faraoni Event show a

$\delta^{13}\text{C}$ response but no unequivocal evidence for widespread black shale deposits.

Over the years, for the Cretaceous system, several multi-million-year records of temporal high-resolution have been generated from the Tethyan Realm, specifically from Italy and SE France (e.g., Weissert et al., 1998; Herrle et al., 2004; Sprovieri et al., 2006; Gyawali et al., 2017). For the Boreal Realm, the Upper Cretaceous is represented by the Chalk successions (e.g., Jenkyns et al., 1994; Mitchell et al., 1996; Jarvis et al., 2006), whereas the Early Cretaceous is almost exclusively covered by bits-and-pieces from the North Sea area, Northern Germany, and the high Arctic (e.g., Mitchell et al., 1996; Rückheim et al., 2006; Bottini and Mutterlose, 2012; Herrle et al., 2015; Möller et al., 2020; Thöle et al., 2020; Eldrett and Vieira, 2022). So far, a comprehensive high-resolution long-term record from the Early Cretaceous of the Boreal Realm is still pending.

In this study, drill sites from the larger Hanover area have been combined to construct an almost complete Boreal record covering the upper Berriasian to the lowermost Coniacian (Figure 1). New datasets, specifically from the Aptian–Albian interval, fill important gaps when comparing the new Boreal composite to another composite record from previously published Tethyan successions of SE France. This kind of Boreal–Tethyan correlation is crucial to resolve long-lasting, general issues, such as floral and faunal endemism, diachronous appearances or extinctions of taxa, and differences in the abundance of biostratigraphic important taxa and taxonomic uncertainties that might hamper a reliable biostratigraphic correlation between the different provinces at a reasonable high resolution.

2 Geological setting

All studied cores and successions are from the eastern central part of the Lower Saxony Basin (LSB). In Early Cretaceous times, the LSB represented a northwest/southeast-oriented sedimentary basin surrounded by the Pompeckj High in the north and the Rhenish Massif in the south (Mutterlose and Bornemann, 2000). Late Jurassic to Cretaceous salt tectonic movements have controlled the spatial sedimentation pattern during the Cretaceous, leading to considerable differences in sequence thicknesses also on small regional scales (Voigt and Wagreich, 2008). Due to the long-term eustatic sea-level rise during the Albian and Cenomanian (Haq, 2014), the Pompeckj Block became inundated, and a large uniform sedimentation area along the epicontinental shelf, the North German Basin (NGB), developed that connected the Tethys in the southeast with the North Sea in the northwest (Voigt and Wagreich, 2008). At the same time, the NGB experienced a lithological change from a siliciclastic-dominated to a carbonate-dominated sedimentary regime. A more detailed description of the basin evolution of North Germany is provided by Mutterlose and Bornemann (2000) and Voigt and Wagreich (2008) and references therein.

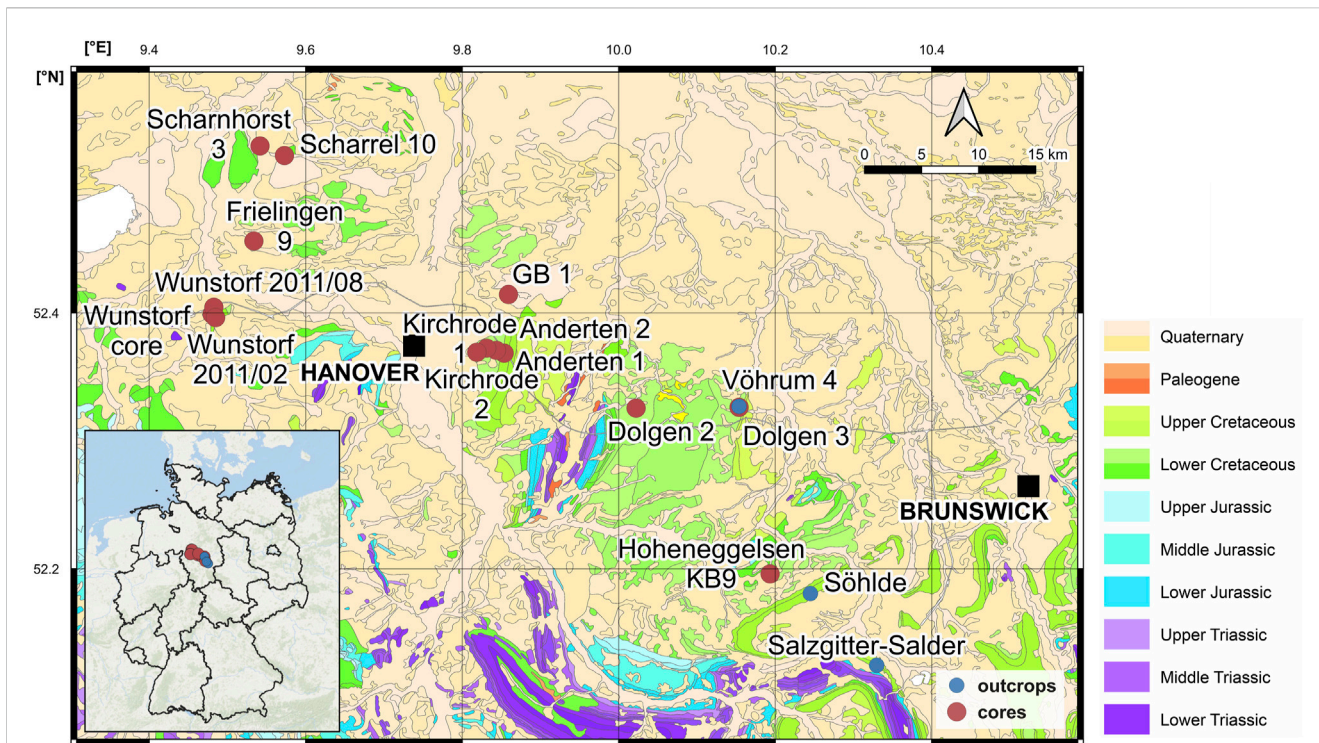


FIGURE 1 Geological map (base layer) of the study area (General Geological Map of the Federal Republic of Germany 1:250,000, GÜK250; BGR, 2019), showing the geographic positions of the studied cores and sections. The inset map shows the positions of the studied successions in Germany.

TABLE 1 Overview of studied or discussed drill cores and outcrops (in stratigraphic order).

Core/outcrop (c/o)	Coordinate (°lon E/°lat N)	Stratigraphic range	Data source
Scharnhorst 3 (c)	9.541632/52.529999	Berriasian–Valanginian	Thöle et al. (2020)
Scharrel 10 (c)	9.572881/52.522544	Valanginian–Hauterivian	Thöle et al. (2020)
Frielingen 9 (c)	9.533782/52.455967	Valanginian–Lower Aptian	Thöle et al. (2020)
Hoheneggelsen KB9 (c)	10.193503/52.196078	Lower Aptian	Bottini and Mutterlose (2012)
Dolgen 2 (c)	10.022247/52.325693	Middle–Upper Aptian	This study
Dolgen 3 (c)	10.153599/52.329202	Upper Aptian–Lower Albian	This study
Vöhrum 4 pit (o)	10.1535/52.32541666	Lower Albian	Mutterlose et al. (2003), Selby et al. (2009)
Kirchrode 2 (c)	9.818667/52.369333	Lower–Upper Albian	Nebe (1999) and this study
Kirchrode 1 (c)	9.831167/52.3725	Upper Albian	J. Thurow and this study
GB-1 (c)	9.859135/52.414389	Middle Albian	Erbacher et al. (2011)
Anderten 1 (c)	9.853563/52.368641	Upper Albian–Lower Cenomanian	Bornemann et al. (2017)
Anderten 2 (c)	9.843592/52.370842	Upper Albian–Lower Cenomanian	Bornemann et al. (2017)
Wunstorf 2011/8 (c)	9.48264/52.40444	Cenomanian	Erbacher et al. (2020)
Wunstorf 2011/2 (c)	9.484863/52.396364	Cenomanian	Erbacher et al. (2020)
Wunstorf core (c)	9.480392/52.39903	Cenomanian–Turonian	Voigt et al. (2008)
Söhlide (o)	10.244923/52.180669	Turonian	Voigt and Hilbrecht (1997)
Salzgitter-Salder (o)	10.329713/52.124373	Turonian–Lower Coniacian	Voigt and Hilbrecht (1997); Voigt et al. (2021)

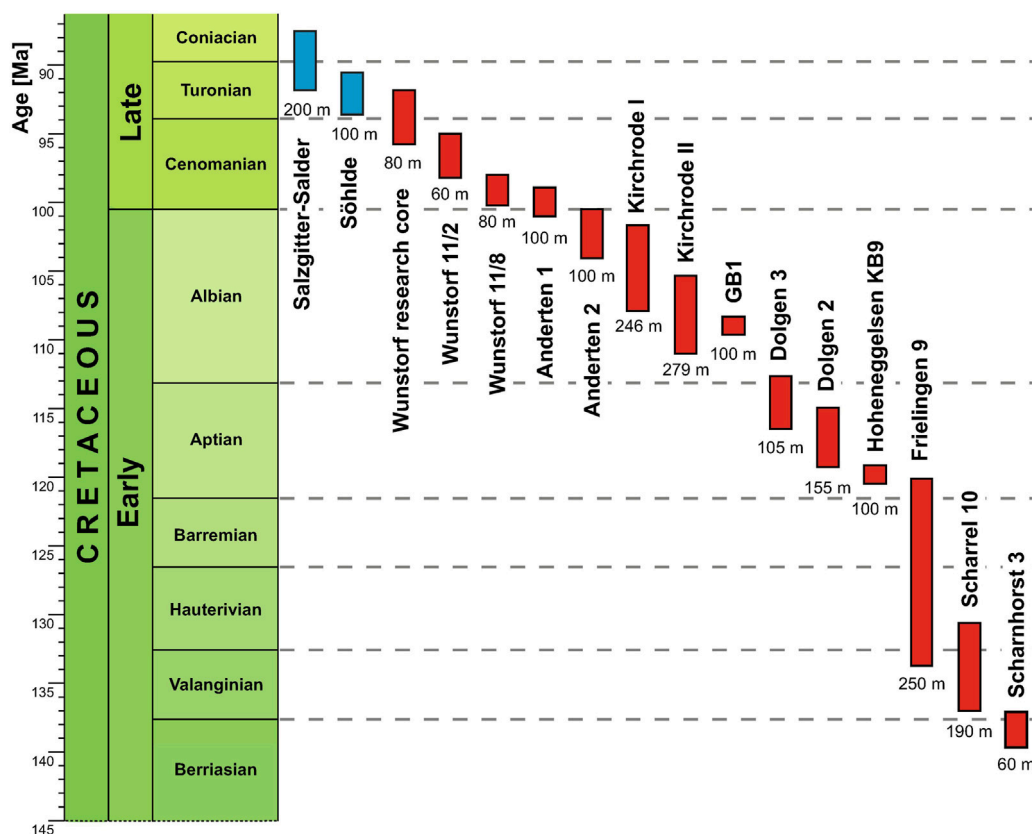


FIGURE 2

Stratigraphic ranges of the studied cores (in red) and outcrops (in blue), including core lengths and section thicknesses. Geological timescale according to GTS 2020 (Gale et al., 2020).

3 Material and methods

More than 5,000 $\delta^{13}\text{C}$ analyses from 14 drill cores and 2 outcrops are presented and compiled in this study, from which more than 800 analyses are from unpublished records (see Table 1; supplementary data). For the upper Berriasian to lower Albian drill cores (Scharnhorst 3, Scharrel 10, Frielingen 9, Hoheneggelsen KB9, Dolgen 2 and 3, lower part of Kirchrode 2; Figure 2; Table 1), $\delta^{13}\text{C}_{\text{org}}$ has been analyzed because of the general low carbonate contents in the Lower Cretaceous sediments (Mutterlose and Bornemann, 2000; Thöle et al., 2020). Based on a palynofacies study by Thöle (2017), the composition of organic particles of the Valanginian to lower Aptian mudstones has been assigned to a heterolithic oxic shelf environment (following the Tyson, 1995, palynofacies classification). Furthermore, the composition of the organic carbon has been considered to be relatively stable throughout this time interval. The geologically younger cores and sections (Table 1; Figure 2), which are characterized by a carbonate content above 20 wt% $\delta^{13}\text{C}$, have been measured on the carbonate fraction ($\delta^{13}\text{C}_{\text{carb}}$). Only for the lower part of Kirchrode 2, both $\delta^{13}\text{C}_{\text{carb}}$ and $\delta^{13}\text{C}_{\text{org}}$ were analyzed.

Many sites of this compilation have previously been published elsewhere, such as the late Berriasian to early Aptian interval by Thöle et al. (2020), the Albian–Cenomanian transition (Bornemann et al., 2017), and the Cenomanian–Turonian transition recorded in

the Wunstorf cores (Voigt et al., 2008; Erbacher et al., 2020). Unpublished data are specifically from the Aptian–Albian interval (Dolgen 2/3 and Kirchrode 1/2). An overview of the studied cores and sections, including the data sources, is given in Table 1. Tie points among the studied cores have been defined based on multiple criteria, including litho-, chemo-, and biostratigraphy, and are documented in Supplementary Table S1.

New $\delta^{13}\text{C}_{\text{org}}$ data from the Dolgen 2/3 and Kirchrode 1/2 cores were analyzed at the Federal Institute for Geosciences and Natural Resources (BGR) after decalcification with HCl, using a ThermoFlash EA 1112 elemental analyzer coupled via a ConFlo IV interface to an Isotope Ratio Mass Spectrometer (Thermo Delta V Advantage). All isotope values are reported in ‰ VPDB. For all $\delta^{13}\text{C}$ analyses, the reproducibility of repeated standard measurements was in all records better than 0.1‰.

As the principle of carbon isotope stratigraphy is largely based on wiggle matching, a good biostratigraphic age control is indispensable for a reliable chemostratigraphic correlation. In order to achieve this, German sections have been dated by calcareous nannofossil biostratigraphy, in addition to other existing biostratigraphic schemes. The applied age model, including new unpublished biostratigraphic datum levels, is listed in Supplementary Table S2.

For the Boreal–Tethys comparison, a composite record of sections from the Vocontian Basin has been compiled based on

published data and stratigraphies (Morales et al., 2013; Montclus; Gréselle et al., 2011; Vergol, La Charce; Hennig et al., 1999; La Charce; Kujau et al., 2012; Vergol; van de Schootbrugge et al., 2000; La Charce, Angles/Vergons; Godet et al., 2006; Angles; Kuhnt et al., 1998; Cassis–La Bédoule, Les Sardons, Camping; Herrle et al., 2004; Serre Chaitieu, Gaubert, Taron dol, Pré-Guittard, Les Oustous, L'Arboudeysse, Col de Palluel; Reichelt, 2005; Serre Amande, Col de Palluel; Bornemann et al., 2005; Col de Palluel; Gale et al., 1996; Mont Risou; Gyawali et al., 2017; Moriez, Hyèges, Angles, Vergons, Lambruisse). Age models for both records from Northern Germany and Southeast France follow the Geological Timescale 2020 (GTS 2020; Gale et al., 2020).

4 Results and discussion

4.1 Factors controlling $\delta^{13}\text{C}$ and their chemostratigraphic significance

If $\delta^{13}\text{C}$ events are reproducible in both terrestrial and marine systems, absolute values, amplitude, and the shape of isotope shifts might vary between these two systems or different sections. Covariance between terrestrial organic and marine records is considered to reflect a significant coupling of the ocean–atmosphere system (e.g., Gröcke et al., 2005), and that between marine $\delta^{13}\text{C}_{\text{carb}}$ and $\delta^{13}\text{C}_{\text{org}}$ is usually interpreted to show that both carbonate and organic matter were derived from oceanic surface water displaying the original $\delta^{13}\text{C}$ composition (e.g., Kump and Arthur, 1999). On the contrary, decoupled $\delta^{13}\text{C}_{\text{carb}}$ and $\delta^{13}\text{C}_{\text{org}}$ records might indicate diagenetic alteration (Meyer et al., 2013; Han et al., 2018).

In carbonates, meteoric waters can alter the carbon isotope signature of the near-surface rocks (Swart and Eberli, 2005). However, this effect is likely neglectable in cored material, but an early diagenetic meteoric influence cannot be fully ruled out. Other early diagenetic processes, such as aragonite–calcite transformation in shallow marine carbonates or degradation of organic carbon and subsequent re-precipitation of secondary carbonate, or burial diagenesis might have an effect on $\delta^{13}\text{C}_{\text{carb}}$ (Wendler, 2013, and references therein). The latter has been considered to be minor in (hemi)pelagic sediments for paleoceanographic and chemostratigraphic studies (e.g., Marshall, 1992; Weissert et al., 2008). However, the addition of isotopically lighter cement in hemipelagic sediments often leads to generally lighter values than in pelagic deposits with higher carbonate contents (Voigt and Hilbrecht, 1997). Moreover, the source of carbonate (biogenic–abiogenic, fossil groups, taxa, detrital) due to vital effects depending upon the calcifying organism and organic matter (marine, non-marine, detrital) has an impact on the absolute values of $\delta^{13}\text{C}$ (e.g., Wefer and Berger, 1991; Hayes, 1993) and, thus, controls data variability and the shape and magnitude of the $\delta^{13}\text{C}$ shifts. Considering the microbial activity, such as sulfate reduction or methanogenesis in organic-rich sediments, is important when interpreting $\delta^{13}\text{C}_{\text{org}}$.

In addition, in semi-restricted epicontinental seas, the carbon isotopic composition of seawater might differ from the open ocean due to a low rate of water exchange and regional control of the analyzed source material. All these factors might influence the shape

and absolute values between different sections and sites within the same basin or on a supra-regional scale. For bulk epicontinental carbonate analyses, a margin of uncertainty of $\sim 1\%$ may be assumed (e.g., Halverson et al., 2005), for species-specific foraminiferal Cenozoic curves $\sim 0.5\%$ (e.g., Cramer et al., 2009). Nevertheless, our record (Figure 3) clearly shows that all major $\delta^{13}\text{C}$ events are outpacing any alteration processes so that they are still prominent features in the records compiled from Northern Germany. However, a diagenetic influence causing minor changes in $\delta^{13}\text{C}$ shifts cannot be fully excluded.

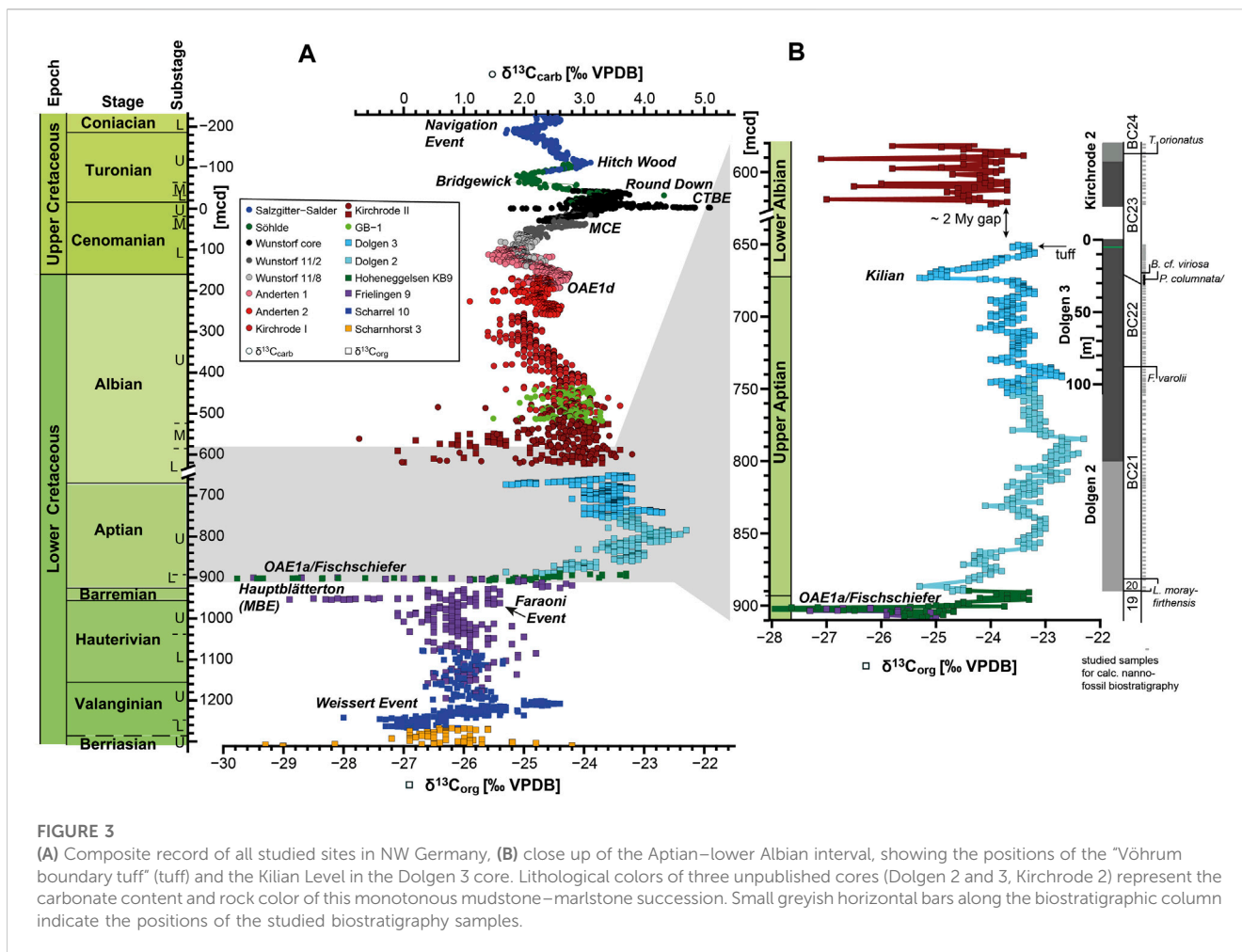
4.2 The German long-term $\delta^{13}\text{C}$ record and its supra-regional significance

A more than 1500-m-thick composite $\delta^{13}\text{C}$ record from Northern Germany has been compiled for the Berriasian to Coniacian interval based on the existing and newly generated stratigraphic framework primarily based on calcareous nannofossils (see Supplementary Table S2) for the studied cores and sections (Figure 3A). The data demonstrate that almost all major carbon isotope perturbations, previously described mostly from low latitudes, are also typical features in semi-restricted basins of the Boreal realm and can thus be considered global chemostratigraphic events. In the following, the key events and their potential causes, identified in the North German composite record, are briefly described.

4.2.1 Valanginian “Weissert Event”

The non-marine upper Berriasian strata are characterized by high variability of $\delta^{13}\text{C}_{\text{org}}$. With the onset of full marine conditions in the early Valanginian, carbon isotope values become more uniform and follow global trends with an earliest Valanginian minimum interval (Figure 4), which is also characteristic of other key records from, for example, SE France (e.g., Martinez et al., 2015; see also Figure 4, and detailed information in the Material and Methods chapter) and the Atlantic Ocean (e.g., Bornemann and Mutterlose, 2008).

In the Scharrel 10 drill core, the $\delta^{13}\text{C}$ values rise from -27% to -24% during the mid-Valanginian (Figure 3A), giving way to the >2.3 My-long (Sprovieri et al., 2006; Martinez et al., 2015) positive $\delta^{13}\text{C}$ excursion of the “Weissert Event” (Erba et al., 2004). The Weissert Event has originally been described from Tethyan successions (Lini et al., 1992; Weissert et al., 1998), as well as from Atlantic and Pacific drill cores (e.g., Erba, 1994; Wortmann and Weissert, 2000). Only recently have the first records of the event been documented from the Boreal Realm (Galloway et al., 2020; Möller et al., 2020; Thöle et al., 2020) and mid-southern latitudes (Cavalheiro et al., 2021). The associated global carbon cycle perturbation was often related to the Parana–Etendeka volcanism and co-occurring carbonate platform drowning (e.g., Wortmann and Weissert, 2000; Martinez et al., 2015). In contrast to younger similar events as the mid-Cretaceous OAEs, the Weissert Event is associated with only minor occurrences of organic-rich sediments. An anoxic interval has recently been identified by Giraldo-Gómez et al. (2022) based on benthic foraminifera faunas at the onset of the Weissert Event in the Weddell Sea, tentatively suggesting that the Southern Ocean might have acted as a potential major carbon sink in



the Valanginian. However, the lack of documented organic carbon-rich rocks of the mid-Valanginian age, possibly due to the incomplete stratigraphic record in many places worldwide, leaves open the role of organic carbon burial in explaining the positive $\delta^{13}\text{C}$ excursion.

4.2.2 Late Hauterivian “Faraoni Event”

In the uppermost Hauterivian of numerous Tethyan successions, a minor black shale bed, the Faraoni Event, has been reported since the mid-1990s (e.g., Cecca et al., 1994; Baudin and Riquier, 2014). The event bed is situated at the base of the maximum of a positive $\delta^{13}\text{C}$ excursion (Martinez et al., 2015), which likely corresponds to ~80 m depth of the Frielingen 9 core (963 mcd; Figure 3A). The stratigraphic position in the Frielingen 9 core is also supported by calcareous nannofossil biostratigraphy. In the Tethys, the Faraoni Event usually corresponds to the last appearance datum (LAD) of *Lithraphidites bollii*, which is situated somewhat below the LAD of *Clepsilolithus maculosus* in the Boreal biozonations, which is in line with our data from the Frielingen 9 core. No major lithological changes are apparent during this interval, but one sample at 80.25 m (963.25 mcd) shows significantly higher TOC values of more than 1 wt% above the background (Thöle et al., 2020). It is hard to judge whether

this level finally represents the Faraoni Event in Northern Germany. However, the chemostratigraphic position is intriguing.

4.2.3 Mid-Barremian Event (Hauptblättertön)

The uppermost Valanginian and Hauterivian show a high $\delta^{13}\text{C}_{\text{org}}$ variability between -27.4‰ and -24.6‰ with a distinct increase in the upper Barremian, directly below a prominent negative excursion of about 3‰ – 4‰ (Figure 3A). The latter is associated with an organic-rich, paper-shale-like clayey deposit named Hauptblättertön in Northern Germany and the Munk Shale in the North Sea area (Mutterlose and Böckel, 1998; Wulff et al., 2020; Ineson et al., 2022). In the Tethys, this Mid-Barremian Event (MBE) is less prominent and shows only a minor expression in $\delta^{13}\text{C}$ of less than -0.5‰ (Coccioni et al., 2003). In the LSB, oxygen deficiency and lamination, indicating the absence of macrobenthic activity, are often explained by thermohaline stratification probably caused by either high surface water temperatures (Mutterlose et al., 2009) or enhanced run-off in this semi-restricted basin or both, leading to a reduced surface water salinity (Mutterlose and Böckel, 1998). For a long time, it has been suggested that this event is associated with a transgressive sea-level trend. However, detailed recent studies by Thöle et al. (2020) and Ineson et al. (2022) found

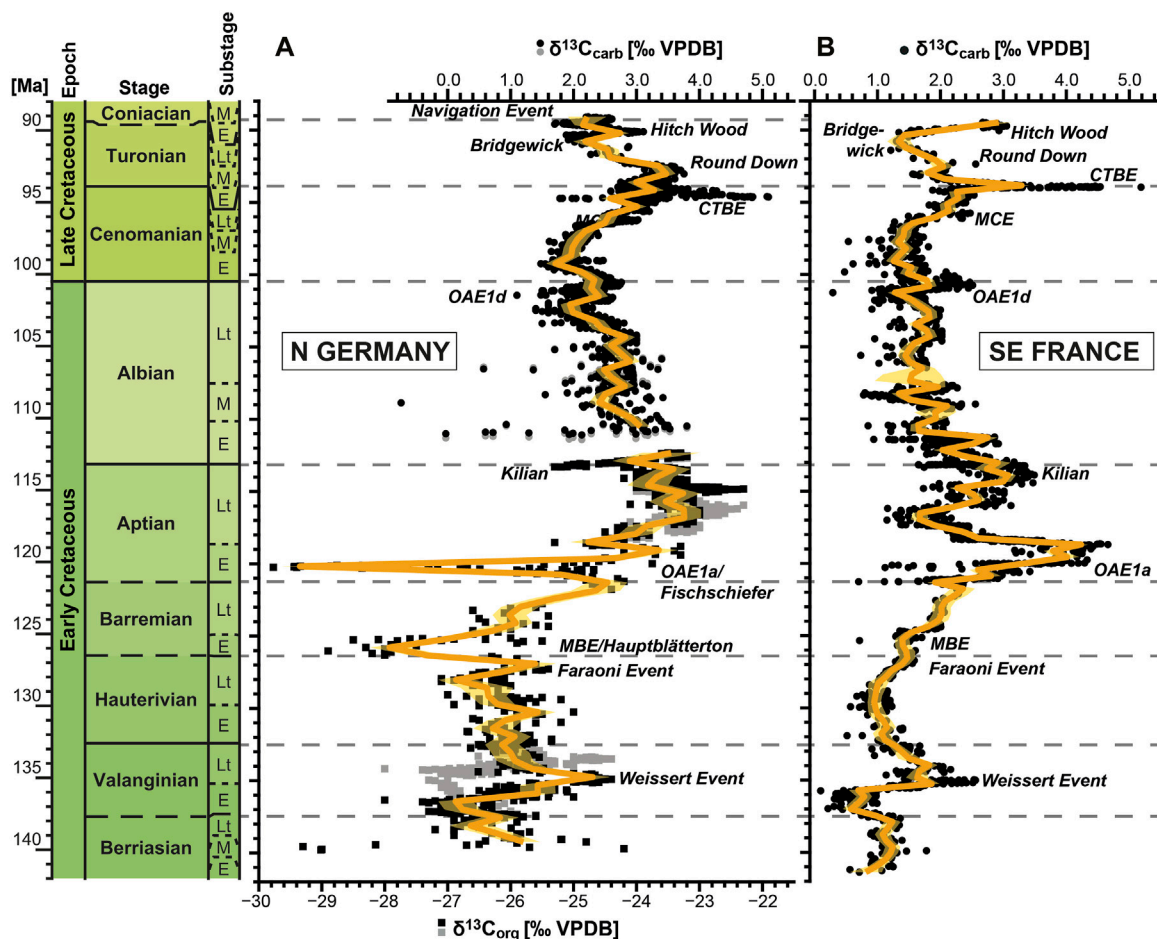


FIGURE 4

Comparison of Northern Germany (A) and SE France (B) composite records plotted against age (GTS 2020, Gale et al. (2020)). For details of the age model for the German sites/sections, see Supplementary Table S2. For Northern Germany, only those data are included within the tie point ranges given in Supplementary Table S1. Furthermore, two records with different age models are shown in (A). Gray symbols represent a primarily calcareous nannofossil-based age model, whereas black symbols represent a chemostratigraphic-adjusted age model, which shows a better match to the Tethyan data in the Valanginian (B). Loess smoothing is indicated by the orange line; the corresponding 95% confidence level is marked by the translucent yellow area.

evidence that the Hauptblättertorn or Munk Shale is characterized by a regressive sea level change in the Boreal. Higher up, $\delta^{13}\text{C}_{\text{org}}$ values steadily increase from -27‰ to -24‰ across the remaining Barremian and until another paper-shale horizon named Fischschiefer, which was deposited in the lower Aptian.

4.2.4 Oceanic Anoxic Event 1a (Fischschiefer)

Beside the OAE 2, the OAE 1a is the most pronounced black shale event and one of the most intensively studied intervals of the Cretaceous. In Northern Germany, this event is lithologically represented by an organic carbon-rich, laminated mudstone (Fischschiefer). Here and in other places worldwide, the OAE 1a is introduced by a sharp negative $\delta^{13}\text{C}$ excursion (in this study, minimum values of -29.7‰) followed by a ~ 1 Myr-lasting positive excursion (e.g., Leandro et al., 2022; in this study maximizing at -23‰ ; Figure 3).

As the primary trigger for this event, the activity of large igneous provinces (LIP) like the High Arctic LIP (Polteau et al., 2016) or the Ontong Java Plateau has been proposed, of which the latter has recently been suggested as more likely (Percival et al., 2021). Carbon modeling suggests that the release of ^{13}C -depleted carbon, maybe thermogenic or biogenic methane from sill intrusions, into the global carbon system has caused a negative spike in deposited $\delta^{13}\text{C}$ (Adloff et al., 2020). Afterward, carbon release might have shifted toward a dominantly more ^{13}C -enriched volcanic source. Furthermore, mantle-derived carbon emissions are also supported by Os isotope data. The following long-term positive excursion is most likely the consequence of the widespread preservation and removal of ^{13}C -depleted organic carbon from the global carbon system. Although the negative peak at the onset of the event is well pronounced in many German sections and cores (Bottini and Mutterlose, 2012; Thöle et al., 2020; this study $>5\text{‰}$ in $\delta^{13}\text{C}_{\text{org}}$), the following positive excursion is rather muted in both $\delta^{13}\text{C}_{\text{carb}}$ and

$\delta^{13}\text{C}_{\text{org}}$ (this study, $\sim 2.5\%$) compared to Tethyan and open ocean data (see discussion; Figure 4).

4.2.5 Kilian Event (Oceanic Anoxic Event 1b)

The 90 to 120 ky-lasting Kilian Event (Leandro et al., 2022) is considered one of the several black shale events associated with the OAE 1b during the Aptian–Albian transition, as defined by Arthur et al. (1990) and Coccioni et al. (2014), especially in the Tethyan realm. Furthermore, the Kilian Event serves as a marker of the Aptian–Albian boundary (Kennedy et al., 2017). In our record, this level is represented by a negative $>1.5\%$ excursion in $\delta^{13}\text{C}_{\text{org}}$ between approximately -23% and -25% (Figure 3B). In addition to the Kilian Event, the lower Albian Paquier Level is another prominent black shale event of the OAE 1b interval, which is not covered by our record and is probably hidden in the early Albian gap. A detailed discussion of the stratigraphy of the Aptian–Albian boundary interval is given in the following paragraph. The cause of these black shale deposits is not well understood. In the past, a number of reasons have been inferred to explain these events, such as the enhanced volcanic activity of the Kerguelen Plateau in the Southern Indian Ocean (Matsumoto et al., 2022), a major transgression during the earliest Albian and enhanced surface ocean stratification during OAE 1b black shale deposition (Erbacher et al., 2001; Herrle et al., 2003).

The remaining lower to lower upper Albian strata are characterized by an interval of high $\delta^{13}\text{C}$ variability that mostly lacks any clear trends over ~ 6 My. Only in the middle upper Albian, a more than -2% $\delta^{13}\text{C}_{\text{carb}}$ decline is observed, followed by the Albian–Cenomanian boundary interval (ACBI). The ACBI consists of up to four positive $\delta^{13}\text{C}$ excursions across this stage boundary and is introduced by the OAE 1d.

4.2.6 Oceanic Anoxic Event 1d and the Albian–Cenomanian boundary interval

The best-studied unequivocal records of the OAE 1d have been documented from SE France (Gale et al., 1996; Br  h  ret, 1997; Bornemann et al., 2005), the Atlantic Ocean (Wilson and Norris, 2001), and recently the southern Indian Ocean (Fan et al., 2022). Similar to the OAE 1b interval, the cause of OAE 1d is not well constrained. In the western North Atlantic, the event has been considered to reflect a major breakdown of surface ocean stratification (Wilson and Norris, 2001). In SE France, it might be associated with orbitally induced changes in nutrient input and stratification changes (Bornemann et al., 2005). In Northern Germany, Bornemann et al. (2017) described the OAE 1d equivalent in the Anderten 1 core, which is part of the composite record presented herein. Evidence is predominantly coming from a sharp negative $\delta^{13}\text{C}_{\text{carb}}$ excursion preceding the long-term ACBI positive excursion resembling the Tethyan records and, to a lesser extent, from enhanced concentrations of reducing elements and the observation of faint lamination.

4.2.7 Mid-Cenomanian Event

Following the ACBI, $\delta^{13}\text{C}_{\text{carb}}$ in the north German composite record increases from 1.4% to 3% culminating in the Mid-Cenomanian Event (MCE). The MCE consists of a double peak within a positive $\delta^{13}\text{C}$ excursion of about 1% (Figure 3A). The MCE has been described from a number of settings in England, France

(Figure 4B), Italy, and the North Atlantic (Paul et al., 1994; Coccioni and Galeotti, 2003; Friedrich et al., 2009; Giraud et al., 2013) and has been previously documented at Wunstorf (Wilmsen, 2007; Erbacher et al., 2020, data used herein). Usually, it is interpreted as a high-productivity event possibly associated with a climatically controlled reorganization of ocean circulation and a shift toward a nutrient-rich deep-water source (Zheng et al., 2016). Furthermore, Batenburg et al. (2016) proposed that the MCE is related to the very long eccentricity cycle of 2.0–2.4 My.

4.2.8 Oceanic Anoxic Event 2

The OAE 2 black shale event, also known as the Cenomanian–Turonian Boundary Event (CTBE), has been globally documented with a pronounced positive $\delta^{13}\text{C}_{\text{carb}}$ excursion. In Wunstorf, the $\delta^{13}\text{C}_{\text{carb}}$ values rise from 1.5% to 5.1% (Figure 3A) with the most negative values at the base of the black shale sequence and subsequently follow the positive event; for details, see Voigt et al. (2008). OAE 2 has been linked to the emplacement of large igneous provinces, most likely the Caribbean–Colombian igneous province (Turgeon and Creaser, 2008; Du Vivier et al., 2014). Intense volcanic activity, in turn, caused massive CO_2 outgassing, leading to global warming (Forster et al., 2007; Papadomanolaki et al., 2022) and enhanced ocean fertilization. The latter is considered to have induced high primary production and oxygen depletion of the oceans, which supported massive global organic carbon preservation on the sea floor (e.g., Blumenberg and Wiese, 2012; Gangl et al., 2019).

4.2.9 Post-OAE 2 carbon isotope events

Between the OAE 2 and the Navigation Event, the youngest observed carbon isotope event in our data, a number of other $\delta^{13}\text{C}$ excursions are evident (Figure 3A)—the Round Down, Glynde, Pewsey, Bridgewick, and Hitch Wood Events—mostly named after regional lithological units in the UK by Gale (1996) and Jarvis et al. (2006). Post-OAE 2 $\delta^{13}\text{C}_{\text{carb}}$ values in our dataset range between 1.6% and 3.5% , with most positive values represented by the positive anomalies of the prominent Round Down and Hitch Wood Events, with a less pronounced Pewsey Event slightly above the Round Down interval. The negative $\delta^{13}\text{C}$ Bridgewick and Navigation Events are also well developed.

The Turonian events are not distinctly related to black shale events but were linked to sea-level changes by Jarvis et al. (2006), Jarvis et al. (2015), and others. Furthermore, a potential orbital forcing of carbon cycle changes by the long eccentricity cycle has been proposed (e.g., Laurin et al., 2014). The Navigation Event marks the base of the Coniacian (Walaszczyk et al., 2021) and is well described from the Boreal sections, specifically at Salzgitter-Salder—the Global Stratigraphic Section and Point (GSSP) for the Turonian–Coniacian boundary. The event has also been identified in SE France and the North Atlantic (Voigt et al., 2021, and references therein).

4.3 Boreal–Tethys comparison

In order to test both the validity of our record and a Boreal–Tethys correlation, a long-term record from SE France has been compiled from previously published datasets (for

details, see the Material and Methods section). Comparing the French record to the one from the LSB reveals various similarities and dissimilarities. Both basins from the different realms display expected $\delta^{13}\text{C}$ responses to the major events, albeit of different magnitudes and excursion shapes. Furthermore, during certain intervals in the LSB record, the data are a bit noisy, and it has to be considered that the compilation for Northern Germany relies on both $\delta^{13}\text{C}_{\text{org}}$ and $\delta^{13}\text{C}_{\text{carb}}$ and that for SE France solely on $\delta^{13}\text{C}_{\text{carb}}$. This together complicates the correlation of some short-term shifts in $\delta^{13}\text{C}$.

During the Berriasian stage in SE France and other low latitudinal successions, the $\delta^{13}\text{C}$ curve is relatively stable below the Valanginian Weissert Event (Weissert and Erba, 2004; Martinez et al., 2015), whereas the LSB data display a high variability. This is probably caused by different aquatic and terrestrial organic carbon sources for $\delta^{13}\text{C}_{\text{org}}$, which have been deposited in the rather small, restricted, non-marine LSB. Blumenberg et al. (2019) observed high abundances of organic compounds of *Botryococcus* algae and sulfur bacteria, but also dinoflagellates, which might have contributed to the high $\delta^{13}\text{C}_{\text{org}}$ variability. The basin became fully marine with a dominant marine organic carbon source after the earliest Valanginian transgression (Mutterlose and Bornemann, 2002), resulting in more uniform $\delta^{13}\text{C}$ values that are well in line with the Tethyan $\delta^{13}\text{C}_{\text{carb}}$ data (Figure 4).

The $\delta^{13}\text{C}$ excursion of the mid-Valanginian Weissert Event and the preceding basal Valanginian minimum is well developed in both records and is of similar magnitude. However, applying the calcareous nannofossil-based age model according to GTS2020 leads to a 1–2 My younger position of the Weissert Event in the LSB compared to the Vocontian Basin record (Figure 4). The Tethyan record that is based on stratotype sections is, therefore, much better stratigraphically constrained, and a comparison between both basins underlines the potential diachrony of biostratigraphic zonations between different marine basins. Therefore, the $\delta^{13}\text{C}$ excursion of the Weissert Event has been used as an additional age tie point (according to Martinez et al., 2015) instead of applying a pure biostratigraphic age model. This example shows that there are still substantial intercalibration issues between the Boreal and Tethyan Realms that can be improved with the help of chemostratigraphy.

Following the Weissert event, the $\delta^{13}\text{C}$ values decrease with decreasing time across the base of the Hauterivian in both realms. A distinct minimum occurs in the basal lower Hauterivian in SE France and is also recorded by the Boreal data. The Hauterivian trend is less clear in the LSB due to a higher data variability. Moreover, the minimum is more discreet and seems to be skewed again toward a younger age by 1–2 My compared to SE France.

The high $\delta^{13}\text{C}$ variability in the Hauterivian might result from various mechanisms. The LSB remained a relatively small and restricted basin with limited water mass exchange with the open ocean during this time interval. Sedimentary $\delta^{13}\text{C}$ from epicontinental seas records carbon from water masses that did not have unrestricted circulation with the ocean (Holmden et al., 1998) and was potentially regionally affected by terrestrial carbon sources. Such a restriction may cause larger amplitudes and higher variability of $\delta^{13}\text{C}$ than the global ocean reservoir.

Thus, pelagic carbonates are likely to record less variability than epicontinental sea carbonates (Saltzman and Thomas, 2012). Such a scenario is supported by numerous phases of Tethyan influence that have been documented for this stage by Mutterlose and Bornemann (2002), suggesting at least episodic openings of gateways to the Tethys. This, in turn, also implies phases of decoupling from the Tethyan system and a stronger impact of local mechanisms controlling the organic carbon $\delta^{13}\text{C}$ due to the input of terrestrial organic matter and primary production. Moreover, the Hauterivian experienced a long-term sea-level rise (Haq, 2014), which might have increased the extension of the LSB. Flooding of large continental areas might also cause a larger influx of different organic carbon sources into the basin, leading to the observed noise in the dataset. However, even if it remains difficult to correlate minor shifts with the Tethyan records, the potential of a high-resolution intrabasinal correlation was demonstrated by Thöle et al. (2020).

A minor positive excursion occurs in both records in the uppermost Hauterivian. At the base of this peak, the Faraoni Event has potentially been observed. This maximum is followed by a pronounced negative shift in $\delta^{13}\text{C}$ associated with the Hauptblättertön in the LSB that is substantially larger than in the Tethys, but, again, it has to be considered that excursions in $\delta^{13}\text{C}_{\text{org}}$ are generally higher than those in $\delta^{13}\text{C}_{\text{carb}}$ (Jenkyns, 2010). This is also evident from Figure 3A when comparing the amplitudes of the $\delta^{13}\text{C}_{\text{org}}$ (Berriasian to lower Albian) and $\delta^{13}\text{C}_{\text{carb}}$ (lower Albian and above) shifts.

The Barremian Hauptblättertön consists of up to 8 wt% of organic carbon in Lower Saxony (Mutterlose and Böckel, 1998; 4 wt% in the Frielingen 9 core, Thöle et al., 2020) and might be prone to early diagenetic alteration due to organic matter degradation by selective preservation of isotopically light lipid-rich and refractory material or metabolic isotope fractionation processes (e.g., Hayes, 1993; Tyson, 1995; Freudenthal et al., 2001). Increased input or selective preservation of terrestrial organic matter, which might also shift $\delta^{13}\text{C}_{\text{org}}$ toward lighter values (e.g., Tyson, 1995), can be ruled out because organic geochemical data by Littke et al. (1998) suggested a dominance of marine organic matter for the Hauptblättertön. This interpretation is in agreement with Mutterlose et al. (2009) and Pauly et al. (2013), who suggest that the negative $\delta^{13}\text{C}$ values previously documented for Hauptblättertön reflect a regional or diagenetic signal in the semi-restricted LSB.

The interval between the Hauptblättertön and the Aptian Fischschiefer displays a steady increase in $\delta^{13}\text{C}$ values, but both records have a very low data resolution. This argues either for low sedimentation rates in both basins or more likely for an age-model artifact due to a recent multi-million-year shift of the Barremian–Aptian boundary in the GTS2020 compared to previous time scales (GTS2012–126.3 Ma, GTS2020–121.4 Ma).

The comparison of the North German record with SE France further demonstrates numerous clear shifts, which stratigraphically differ from each other during the upper Aptian and Albian. Both intervals are characterized by outstanding longevity of many biozones of calcareous nannofossils, planktic foraminifera, and ammonites in both the Tethys and Boreal, which often last for several million years. In addition, a reliable stratigraphy framework

is also hampered by the lack of geomagnetic reversals during the Cretaceous Normal Superchron interval (e.g., Ogg, 2020). This results in a high degree of stratigraphic uncertainties, making it difficult to reliably constrain the stratigraphic position and the duration of $\delta^{13}\text{C}$ shifts, which becomes apparent in the Boreal–Tethys correlation (Figure 4).

$\delta^{13}\text{C}_{\text{carb}}$ is showing a high variability of up to 4‰ in the lower to lowermost upper Albian and of 1‰–1.5‰ above, superimposed by a million-year long-term trend to lighter values in the upper Albian, but without any unequivocal short-term trends. The large data spread is not unique to the $\delta^{13}\text{C}_{\text{carb}}$ records from the Kirchrode I and II cores but is also apparent in the $\delta^{13}\text{C}_{\text{org}}$ data and supported by the GB-1 core. GB-1 has not been included in the long-term record because it fully overlaps with the Kirchrode cores, but both records show the same high variability (Figure 3). Similar to the Hauterivian, we speculate that the combination of a major sea-level rise and the input of various carbon sources either from the leached hinterland or episodic mixing with other water masses might have contributed to the high data variability. However, in Albian times, the LSB has evolved toward the North German Basin with a continuous, relatively wide connection to the proto-North Sea (Mutterlose and Bornemann, 2000).

Finally, in both records, the ACBI with the OAE 1d at its base has been identified (see also Bornemann et al., 2017). During the remaining Late Cretaceous, the observed trends and excursions are very similar without any apparent stratigraphic discrepancies between the LSB, the Tethys, and the English chalk reference curve (Jarvis et al., 2006); nevertheless, the magnitudes of the excursions are somewhat different. To summarize, as the major events are all present in the presented records, it is unlikely that diagenesis or regional differences in the composition of bulk organic carbon are significant factors controlling the long-term changes in $\delta^{13}\text{C}_{\text{carb}}$ and $\delta^{13}\text{C}_{\text{org}}$ in the studied succession.

4.4 New stratigraphic implications for the Aptian–Albian boundary interval

The Aptian–Albian interval of the Dolgen 3 core provides new, crucial results for the stratigraphic position of this stage boundary in the Boreal realm. The clayey sediments of this interval are poor in carbonate (Schwieldt-Subformation), and calcareous plankton is usually rare and partly dissolved. This often hampers the biostratigraphic assignments of some samples. Due to provincialism, classical ammonite stratigraphy is hard to correlate with Tethyan records (Mutterlose et al., 2003; Mutterlose et al., 2009). A tuff horizon at Vöhrum, once proposed as a GSSP marker bed for the Aptian–Albian boundary (Mutterlose et al., 2003), has been dated at 113.1 ± 0.3 Ma using $^{206}\text{Pb}/^{238}\text{U}$ (Selby et al., 2009), which is why the Aptian–Albian boundary is currently placed at 113.2 Ma since the Geological Timescale 2016 has been released. However, due to the outcrop conditions at the Vöhrum 4 section, the record presented by Mutterlose et al. (2003) is limited and does not allow identifying other events typical for the Aptian–Albian transition elsewhere; also, globally accepted microfossil markers for the Aptian–Albian boundary event have not been documented.

In this study, we present new stable isotope and biostratigraphic data from the Dolgen 3 drill core (Lenz et al., 1986), which was drilled ~500 m north of the Vöhrum 4 pit (Figure 1). Dolgen 3 covers both the mentioned tuff horizon close to its top (5.2 m) and the $\delta^{13}\text{C}$ excursion representing the Kilian Event (onset at 26.49 m) that marks the Aptian–Albian boundary (Kennedy et al., 2017). In this core, the event is represented by a negative >1.5‰ excursion and biostratigraphic changes that resemble Tethyan records (Kennedy et al., 2017) (Figure 3). Biostratigraphically, the stage boundary is defined by planktic foraminifera with the first appearance datum (FAD) of *Microhedbergella renilaevs*, which are not studied herein, and approximated by the FAD of the calcareous nannofossil *Prediscosphaera columnata* (base BC23, Bown et al., 1998; Kennedy et al., 2017). The latter has been observed right at the excursion (24.67 m), but the real FAD might be potentially slightly below the Kilian Event due to a lack of calcareous nannofossils between 31 and 25 m (Bornemann, 2020). This occurrence is directly followed by the FAD of *Broinsonia viriosa*, showing that the development of events is similar to the observations from the Col de Pré Guittard, the approved GSSP for the Aptian–Albian boundary (Kennedy et al., 2017). These findings document for the first time the Aptian–Albian boundary in the Boreal realm.

Both chemo- and biostratigraphic data from the Dolgen 3 core suggest that the Vöhrum tuff is well situated in the lower Albian, questioning the applicability of the $^{206}\text{Pb}/^{238}\text{U}$ age of 113.1 ± 0.3 Ma by Selby et al. (2009) as a reference for the correct age for the Aptian–Albian boundary. There are 20 m of core between the tuff horizon and the peak of the $\delta^{13}\text{C}$ excursion. Considering an average sedimentation rate of 3.62 ± 0.08 cm/ky for this interval as delineated from BC calcareous nannofossil datum levels (according to Bown et al., 1998) and their ages given by GTS 2020 (base BC21: 118.83 Ma, mid-point: 881.46 ± 1.2 mcd; base BC23: 113.17 Ma, mid-point: 676.34 ± 3.5 mcd), the Kilian Event might be 552 ± 13 ky older than the tuff bed.

This sedimentation rate is similar to the 3.84 cm/ky suggested by Nebe (1999) based on a cyclostratigraphic analysis of the lowermost part of Kirchrode 2 (lower Albian), which is located ~20 km further west. This represents a rather conservative estimate as Nebe (1999) also studied two additional cores with sedimentation rates between 2.69 cm/ky (Hoheneggelsen KB52) and 3.03 cm/ky (Hoheneggelsen KB36), which are situated ~10 km south of the Dolgen 3 drill site. Both would result in an even older age for the boundary. However, a ~500 ky age offset can also be derived by comparing our $\delta^{13}\text{C}$ data to the $\delta^{13}\text{C}_{\text{carb}}$ changes at the top of the Poggio le Guaine core (Italy, Leandro et al., 2022). We, therefore, tentatively suggest an Aptian–Albian boundary age of c. 113.65 Ma instead of 113.2 Ma (Gale et al., 2020).

Finally, a lower Albian gap has been identified in our record between the top of Dolgen 3 and the base of Kirchrode 2 cores. The gap duration has been estimated by about 2 My based on cyclostratigraphically derived average sedimentation rates as given by Nebe (1999) for the basal Kirchrode 2 core and the GTS2020 age of base BC24 (109.96 Ma) as observed in the Kirchrode 2 core and the age of the tuff in Vöhrum 4 (Selby et al., 2009). This seems to be the only apparent gap in the long-term record besides an interval of potentially low sedimentation during the lower Aptian.

5 Conclusion

A high-resolution $\delta^{13}\text{C}$ stratigraphy is presented for the LSB in Northern Germany, covering the Berriasian to Coniacian stages (c. 142–88 Ma). This composite record based on 14 drill cores and 2 outcrops is correlated with a Tethyan reference compilation of the Vocontian Basin in SE France. The new boreal reference curve record can be considered almost complete except for a likely 2-Myr gap in the early Albian.

Most of the major global $\delta^{13}\text{C}$ events, such as the Weissert Event, the Aptian–Albian OAEs 1a/b/d, and the Cenomanian–Turonian OAE 2, among many others, are present in the record and serve as useful tie points for supra-regional stratigraphic correlations. Based on this, some biostratigraphic inconsistencies between the LSB and SE France are pointed out for the mid-Valanginian, that is, the position of the Weissert Event, and the late Aptian–Albian interval. Furthermore, some carbon isotope events are recorded for the first time in Northern Europe, such as the Kilian Event and likely the Faraoni Event. The Kilian Event, which represents the Aptian–Albian boundary, allowed for the correct positioning of the boundary in the Boreal realm. The stratigraphic position of the Vöhrum boundary tuff and the age of the boundary could be better constrained, suggesting a boundary age that might be slightly older with c. 113.65 Ma than the official age of 113.2 Ma.

Data availability statement

The raw data supporting the conclusion of this article will be made available by the authors without undue reservation.

Author contributions

AB and JE designed the study, conducted the main analysis, and wrote the bulk of the manuscript. MB conducted most of the analyses. SV provided data and stratigraphic information for the Upper Cretaceous. MB and SV were involved in discussions and

manuscript writing. All authors contributed to the article and approved the submitted version.

Acknowledgments

The authors thank T. Kollaske (BGR) for core handling and support during various sampling sessions. They also thank M. Heldt (BGR) for sampling the Dolgen 2 core and J. Thurow (UCL) for providing them with isotope data from the Kirchröde cores. They thank G. Grützner and S. Stäger (both BGR) for SEM imaging and sample preparation and P. Adam, A. Freiberg, S. Kramer, Y. Meve, and G. Scheeder (all BGR) for $\delta^{13}\text{C}_{\text{org}}$ analyses. The authors further thank Greg Price and Irene Cornacchia for their constructive and insightful reviews.

Conflict of interest

The authors declare that the research was conducted in the absence of any commercial or financial relationships that could be construed as a potential conflict of interest.

Publisher's note

All claims expressed in this article are solely those of the authors and do not necessarily represent those of their affiliated organizations or those of the publisher, the editors, and the reviewers. Any product that may be evaluated in this article, or claim that may be made by its manufacturer, is not guaranteed or endorsed by the publisher.

Supplementary material

The Supplementary Material for this article can be found online at: <https://www.frontiersin.org/articles/10.3389/feart.2023.1173319/full#supplementary-material>

References

- Adloff, M., Greene, S. E., Parkinson, I. J., Naafs, B. D. A., Preston, W., Ridgwell, A., et al. (2020). Unravelling the sources of carbon emissions at the onset of Oceanic Anoxic Event (OAE) 1a. *Earth Planet. Sci. Lett.* 530, 115947. doi:10.1016/j.epsl.2019.115947
- Arthur, M. A., Brumsack, H.-J., Jenkyns, H. C., and Schlanger, S. O. (1990). "Stratigraphy, geochemistry, and paleoceanography of organic carbon-rich Cretaceous sequences," in *Cretaceous Resources, events and rhythms: Background and plans for research*. Editors R. N. Ginsburg and B. Beaudoin (Dordrecht: Springer Netherlands), 75–119. doi:10.1007/978-94-015-6861-6_6
- Batenburg, S. J., Friedrich, O., Moriya, K., Voigt, S., Cournède, C., Moebius, I., et al. (2018). Late Maastrichtian carbon isotope stratigraphy and cyclostratigraphy of the Newfoundland Margin (site U1403, IODP leg 342). *Newsletters Stratigr.* 51 (2), 245–260. doi:10.1127/nos/2017/0398
- Batenburg, S. J., Vleeschouwer, D. D., Sprovieri, M., Hilgen, F. J., Gale, A. S., Singer, B. S., et al. (2016). Orbital control on the timing of oceanic anoxia in the Late Cretaceous. *Clim. Past* 12, 1995–2009. doi:10.5194/cp-12-1995-2016
- Baudin, F., and Riquier, L. (2014). The late Hauterivian Faraoni 'oceanic anoxic event': An update. *Bull. Société Géologique Fr.* 185, 359–377. doi:10.2113/gssgfbull.185.6.359
- BGR (2019). Geologische Übersichtskarte der Bundesrepublik Deutschland 1000 (GÜK250, WMS). *Science* 1, 250.
- Blumenberg, M., and Wiese, F. (2012). Imbalanced nutrients as triggers for black shale formation in a shallow shelf setting during the OAE 2 (Wunstorf, Germany). *Biogeosciences* 9, 4139–4153. doi:10.5194/bg-9-4139-2012
- Blumenberg, M., Zink, K. G., Scheeder, G., Ostertag-Henning, C., and Erbacher, J. (2019). Biomarker paleo-reconstruction of the German Wealden (Berriasian, Early Cretaceous) in the Lower Saxony Basin (LSB). *Int. J. Earth Sci. Geol. Rundsch* 108, 229–244. doi:10.1007/s00531-018-1651-5
- Bornemann, A. (2020). Biostratigraphischer Bericht zur Bohrung Dolgen 3 (3626GE0010) (kalkige Nannofossilien). *Landesamt für Bergbau, Energie und Geologie*. doi:10.48476/PSL_6099_7603
- Bornemann, A., Erbacher, J., Heldt, M., Kollaske, T., Wilmsen, M., Lübke, N., et al. (2017). The Albian-Cenomanian transition and oceanic anoxic event 1d - an example from the boreal realm. *Sedimentology* 64, 44–65. doi:10.1111/sed.12347
- Bornemann, A., and Mutterlose, J. (2008). Calcareous nannofossil and $\delta^{13}\text{C}$ records from the early cretaceous of the Western Atlantic Ocean: Evidence for enhanced fertilization across the Berriasian-Valanginian transition. *PALAIOS* 23, 821–832. doi:10.2110/palo.2007.p07-076r
- Bornemann, A., Pross, J., Reichelt, K., Herrle, J. O., Hemleben, C., and Mutterlose, J. (2005). Reconstruction of short-term palaeoceanographic changes during the formation of the late Albian "Niveau Breistroffer" black shales (oceanic anoxic event 1d, SE France). *J. Geol. Soc.* 162, 623–639. doi:10.1144/0016-764903-171

- Bottini, C., and Mutterlose, J. (2012). Integrated stratigraphy of early Aptian black shales in the boreal realm: Calcareous nannofossil and stable isotope evidence for global and regional processes. *Newsletters Stratigr.* 45, 115–137. doi:10.1127/0078-0421/2012/0017
- Bown, P. R., Rutledge, D. C., Crux, J. A., and Gallagher, L. T. (1998). “Lower cretaceous,” in *Calcareous nannofossil biostratigraphy*. Editor P. R. Bown (Dordrecht, Boston, London: Kluwer Academic Publishers), 86–131.
- Bréhéret, J.-G. (1997). *L’Aptien et l’Albien de la Fosse vocontienne (des bordures au bassin), Evolution de la sédimentation et enseignements sur les événements anoxiques*. Berlin: Springer.
- Cavalheiro, L., Wagner, T., Steinig, S., Bottini, C., Dummman, W., Esegue, O., et al. (2021). Impact of global cooling on Early Cretaceous high pCO₂ world during the Weissert Event. *Nat. Commun.* 12, 5411. doi:10.1038/s41467-021-25706-0
- Cecca, F., Pallini, G., Erba, E., Premoli-Silva, I., and Coccioni, R. (1994). Hauterivian-Barremian chronostratigraphy based on ammonites, nannofossils, planktonic-foraminifera and magnetic chrons from the Mediterranean domain. *Cretac. Res.* 15, 457–467. doi:10.1006/cres.1994.1027
- Coccioni, R., Galeotti, S., and Sprovieri, M. (2003). *The mid-barremian event (MBE): The prelude to the OAE1a*. Berlin: Springer.
- Coccioni, R., and Galeotti, S. (2003). The mid-cenomanian event: Prelude to OAE 2. *Palaeoogeogr. Palaeoclimatol. Palaeoecol.* 190, 427–440. doi:10.1016/s0031-0182(02)00617-x
- Coccioni, R., Sabatino, N., and Frontalini, F. (2014). The neglected history of oceanic anoxic event 1b: Insights and new data from the Poggio le Guaine section (Umbria–Marche basin). *Stratigraphy* 2014, 1–10.
- Cramer, B. S., Toggweiler, J. R., Wright, J. D., Katz, M. E., and Miller, K. G. (2009). Ocean overturning since the Late Cretaceous: Inferences from a new benthic foraminiferal isotope compilation. *Paleoceanography* 24, PA4216. doi:10.1029/2008pa001683
- Du Vivier, A. D. C., Selby, D., Sageman, B. B., Jarvis, I., Gröcke, D. R., and Voigt, S. (2014). Marine ¹⁸⁷Os/¹⁸⁸Os isotope stratigraphy reveals the interaction of volcanism and ocean circulation during Oceanic Anoxic Event 2. *Earth Planet. Sci. Lett.* 389, 23–33. doi:10.1016/j.epsl.2013.12.024
- Eldrett, J. S., and Vieira, M. (2022). An integrated carbon isotope and bio-sequence stratigraphic study of the Early Cretaceous to Paleogene, Central North Sea. *Mar. Petroleum Geol.* 141, 105696. doi:10.1016/j.marpetgeo.2022.105696
- Erba, E., Bartolini, A., and Larson, R. L. (2004). Valanginian Weissert oceanic anoxic event. *Geology* 32, 149–152. doi:10.1130/g20008.1
- Erba, E. (1994). Nannofossils and superplumes - the Early Aptian nannoconid crisis. *Paleoceanography* 9, 483–501. doi:10.1029/94pa00258
- Erba, E. (2006). The first 150 million years history of calcareous nannoplankton: Biosphere-geosphere interactions. *Palaeoogeogr. Palaeoclimatol. Palaeoecol.* 232, 237–250. doi:10.1016/j.palaeo.2005.09.013
- Erbacher, J., Bornemann, A., Petrizzo, M. R., and Huck, S. (2020). Chemostratigraphy and stratigraphic distribution of keeled planktonic foraminifera in the Cenomanian of the North German Basin. *Z. Dtsch. Ges. für Geowiss.* 171, 149–161. doi:10.1127/zdgg/2020/0211
- Erbacher, J., Friedrich, O., Wilson, P. A., Birch, H., and Mutterlose, J. (2005). Stable organic carbon isotope stratigraphy across oceanic anoxic event 2 of Demerara Rise, Western tropical Atlantic. *Geochem. Geophys. Geosystems* 6, 850. doi:10.1029/2004GC000850
- Erbacher, J., Friedrich, O., Wilson, P. A., Lehmann, J., and Weiss, W. (2011). Short-term warming events during the boreal Albian (mid-Cretaceous). *Geology* 39, 223–226. doi:10.1130/G31606.1
- Erbacher, J., Huber, B. T., Norris, R. D., and Markey, M. (2001). Increased thermohaline stratification as a possible cause for an ocean anoxic event in the Cretaceous period. *Nature* 409, 325–327. doi:10.1038/35053041
- Erbacher, J., Thurow, J., and Littke, R. (1996). Evolution patterns of radiolaria and organic matter variations: A new approach to identify sea-level changes in mid-cretaceous pelagic environments. *Geology* 24, 499–502. doi:10.1130/0091-7613(1996)024<0499:epora>2.3.co;2
- Fan, Q., Xu, Z., MacLeod, K. G., Brumsack, H., Li, T., Chang, F., et al. (2022). First record of oceanic anoxic event 1d at southern high latitudes: Sedimentary and geochemical evidence from International Ocean Discovery Program expedition 369. *Geophys. Res. Lett.* 49, 641. doi:10.1029/2021GL097641
- Forster, A., Schouten, S., Moriya, K., Wilson, P. A., and Sinninghe-Damsté, J. S. (2007). Tropical warming and intermittent cooling during the Cenomanian/Turonian Oceanic Anoxic Event 2: Sea surface temperature records from the equatorial Atlantic. *Paleoceanography* 22, 1349. doi:10.1029/2006pa001349
- Freudenthal, T., Wagner, T., Wenzhöfer, F., Zabel, M., and Wefer, G. (2001). Early diagenesis of organic matter from sediments of the eastern subtropical Atlantic: Evidence from stable nitrogen and carbon isotopes. *Geochimica Cosmochimica Acta* 65, 1795–1808. doi:10.1016/S0016-7037(01)00554-3
- Friedrich, O., Erbacher, J., Wilson, P. A., Moriya, K., and Mutterlose, J. (2009). Paleoenvironmental changes across the mid cenomanian event in the tropical Atlantic Ocean (Demerara Rise, ODP leg 207) inferred from benthic foraminiferal assemblages. *Mar. Micropaleontol.* 71, 28–40. doi:10.1016/j.marmicro.2009.01.002
- Gale, A. S., Kennedy, W. J., Burnett, J. A., Caron, M., and Kidd, B. E. (1996). The late Albian to early Cenomanian succession at Mont Risou near Rosans (Drome, SE France): An integrated study (ammonites, inoceramids, planktonic foraminifera, nannofossils, oxygen and carbon isotopes). *Cretac. Res.* 17, 515–606. doi:10.1006/cres.1996.0032
- Gale, A. S., Mutterlose, J., Batenburg, S. J., Gradstein, F. M., Agterberg, F. P., Ogg, J. G., et al. (2020). The Cretaceous period. *Geol. Time Scale* 2020, 1023–1086. doi:10.1016/B978-0-12-824360-2.00027-9
- Gale, A. S. (1996). Turonian correlation and sequence stratigraphy of the Chalk in southern England. *Sequence Stratigr. Br. Geol.* 103, 177–195. doi:10.1144/gsl.sp.1996.103.01.10
- Galloway, J. M., Vickers, M. L., Price, G. D., Poulton, T., Grasby, S. E., Hadlari, T., et al. (2020). Finding the VOICE: Organic carbon isotope chemostratigraphy of late Jurassic – early Cretaceous Arctic Canada. *Geol. Mag.* 157, 1643–1657. doi:10.1017/S0016756819001316
- Gangl, S. K., Moy, C. M., Stirling, C. H., Jenkyns, H. C., Crampton, J. S., Clarkson, M. O., et al. (2019). High-resolution records of Oceanic Anoxic Event 2: Insights into the timing, duration and extent of environmental perturbations from the palaeo-South Pacific Ocean. *Earth Planet. Sci. Lett.* 518, 172–182. doi:10.1016/j.epsl.2019.04.028
- Giraldo-Gómez, V. M., Petrizzo, M. R., Bottini, C., Möller, C., Wagner, T., Cavalheiro, L., et al. (2022). Bottom water redox dynamics during the early cretaceous Weissert event in ODP hole 692B (Weddell Sea, Antarctica) reconstructed from the benthic foraminiferal assemblages. *Palaeoogeogr. Palaeoclimatol. Palaeoecol.* 587, 110795. doi:10.1016/j.palaeo.2021.110795
- Giraud, F., Reboulet, S., Deconinck, J. F., Martinez, M., Carpentier, A., and Bréziat, C. (2013). The Mid-Cenomanian Event in southeastern France: Evidence from palaeontological and clay mineralogical data. *Cretac. Res.* 46, 43–58. doi:10.1016/j.cretres.2013.09.004
- Godet, A., Bodin, S., Föllmi, K. B., Vermeulen, J., Gardin, S., Fiet, N., et al. (2006). Evolution of the marine stable carbon-isotope record during the early cretaceous: A focus on the late hauterivian and barremian in the tethyan realm. *Earth Planet. Sci. Lett.* 242, 254–271. doi:10.1016/j.epsl.2005.12.011
- Gréselle, B., Pittet, B., Mattioli, E., Joachimski, M., Barbarin, N., Riquier, L., et al. (2011). The valanginian isotope event: A complex suite of palaeoenvironmental perturbations. *Palaeoogeogr. Palaeoclimatol. Palaeoecol.* 306, 41–57. doi:10.1016/j.palaeo.2011.03.027
- Gröcke, D., Price, G., Robinson, S., Baraboshkin, E., Mutterlose, J., and Ruffell, A. (2005). The Upper Valanginian (Early Cretaceous) positive carbon-isotope event recorded in terrestrial plants. *Earth Planet. Sci. Lett.* 240, 495–509. doi:10.1016/j.epsl.2005.09.001
- Gyawali, B. R., Nishi, H., Takashima, R., Herrle, J. O., Takayanagi, H., Latil, J.-L., et al. (2017). Upper Albian–upper Turonian calcareous nannofossil biostratigraphy and chemostratigraphy in the Vocontian Basin, southeastern France. *Newsletters Stratigr.* 50, 111–139. doi:10.1127/nos/2016/0339
- Halverson, G. P., Hoffman, P. F., Schrag, D. P., Maloof, A. C., and Rice, A. H. N. (2005). Toward a Neoproterozoic composite carbon-isotope record. *Geol. Soc. Am. Bull.* 117, 1181. doi:10.1130/B25630.1
- Han, Z., Hu, X., Kemp, D. B., and Li, J. (2018). Carbonate-platform response to the Toarcian Oceanic Anoxic Event in the southern hemisphere: Implications for climatic change and biotic platform demise. *Earth Planet. Sci. Lett.* 489, 59–71. doi:10.1016/j.epsl.2018.02.017
- Haq, B. U. (2014). Cretaceous eustasy revisited. *Glob. Planet Change* 113, 44–58. doi:10.1016/j.gloplacha.2013.12.007
- Hayes, J. M. (1993). Factors controlling ¹³C contents of sedimentary organic compounds: Principles and evidence. *Mar. Geol.* 113, 111–125. doi:10.1016/0025-3227(93)90153-M
- Hennig, S., Weissert, H., and Bulot, L. (1999). C-isotope stratigraphy, a calibration tool between ammonite and magnetostratigraphy: The Valanginian-Hauterivian transition. *Geol. Carpathica* 50, 91–95.
- Herrle, J. O., Kossler, P., Friedrich, O., Erlenkeuser, H., and Hemleben, C. (2004). High-resolution carbon isotope records of the aptian to lower Albian from SE France and the mazagan plateau (DSDP site 545): A stratigraphic tool for paleoceanographic and paleobiologic reconstruction. *Earth Planet. Sci. Lett.* 218, 149–161. doi:10.1016/s0012-821x(03)00646-0
- Herrle, J. O., Pross, J., Friedrich, O., and Hemleben, C. (2003). Short-term environmental changes in the Cretaceous Tethyan ocean: Micropaleontological evidence from the early albian oceanic anoxic event 1b. *Terra nova.* 15, 14–19. doi:10.1046/j.1365-3121.2003.00448.x
- Herrle, J. O., Schroder-Adams, C. J., Davis, W., Pugh, A. T., Galloway, J. M., and Fath, J. (2015). Mid-cretaceous high arctic stratigraphy, climate, and oceanic anoxic events. *Geology* 43, 403–406. doi:10.1130/g36439.1
- Holmden, C., Creaser, R. A., Muehlenbachs, K., Leslie, S. A., and Bergström, S. M. (1998). Isotopic evidence for geochemical decoupling between ancient epeiric seas and bordering oceans: Implications for secular curves. *Geol.* 26, 567. doi:10.1130/0091-7613(1998)026<0567:IEFGDB>2.3.CO;2

- Huck, S., Heimhofer, U., Rameil, N., Bodin, S., and Immenhauser, A. (2011). Strontium and carbon-isotope chronostratigraphy of Barremian–Aptian shoal-water carbonates: Northern Tethyan platform drowning predates OAE 1a. *Earth Planet. Sci. Lett.* 304, 547–558. doi:10.1016/j.epsl.2011.02.031
- Ineson, J. R., Lauridsen, B. W., Lode, S., Sheldon, E., Sørensen, H. O., Wisshak, M., et al. (2022). A condensed chalk–marl succession on an Early Cretaceous intrabasinal structural high, Danish Central Graben: Implications for the sequence stratigraphic interpretation of the Munk Marl Bed. *Sediment. Geol.* 440, 106234. doi:10.1016/j.sedgeo.2022.106234
- Jarvis, I., Gale, A. S., Jenkyns, H. C., and Pearce, M. A. (2006). Secular variation in late cretaceous carbon isotopes: A new $\delta^{13}\text{C}$ carbonate reference curve for the cenomanian–campanian (99.6–70.6 Ma). *Geol. Mag.* 143, 561–608. doi:10.1017/s0016756806002421
- Jarvis, I., Trabucchi-Alexandre, J., Gröcke, D. R., Uličný, D., and Laurin, J. (2015). Intercontinental correlation of organic carbon and carbonate stable isotope records: Evidence of climate and sea-level change during the turonian (cretaceous). *Depositional Rec.* 1, 53–90. doi:10.1002/dep2.6
- Jenkyns, H. C., Gale, A. S., and Corfield, R. M. (1994). Carbon- and oxygen-isotope stratigraphy of the English Chalk and Italian Scaglia and its palaeoclimatic significance. *Geol. Mag.* 131, 1–34. doi:10.1017/s0016756800010451
- Jenkyns, H. C. (2010). Geochemistry of oceanic anoxic events. *Geochem. Geophys. Geosystems* 11, 2788. doi:10.1029/2009GC002788
- Jenkyns, H. C. (2018). Transient cooling episodes during cretaceous oceanic anoxic events with special reference to OAE 1a (early aptian). *Phil. Trans. R. Soc. A* 376, 20170073. doi:10.1098/rsta.2017.0073
- Kennedy, J., Gale, A., Huber, B., Pettrizzo, M., Bown, P., Jenkyns, H., et al. (2017). The global boundary stratotype section and point (GSSP) for the base of the albian stage, of the cretaceous, the Col de Pré-guitard section, armayon, drôme, France. *Episodes* 40, 177–188. doi:10.18814/epiugs/2017/v40i3/017021
- Kim, J.-E., Westerhold, T., Alegret, L., Drury, A. J., Röhl, U., and Griffith, E. M. (2022). Precessional pacing of tropical ocean carbon export during the Late Cretaceous. *Clim. Past.* 18, 2631–2641. doi:10.5194/cp-18-2631-2022
- Kuhnt, W., Moullade, M., Masse, J.-P., and Erlenkeuser, H. (1998). Carbon isotope stratigraphy of the lower Aptian petrostratotype at Cassis-La Bédoule (SE France). *Géologie Méditerranéenne* 25, 63–79. doi:10.3406/geolm.1998.1625
- Kujau, A., Heimhofer, U., Ostertag-Henning, C., Gréselle, B., and Mutterlose, J. (2012). No evidence for anoxia during the Valanginian carbon isotope event - an organic-geochemical study from the Vocontian Basin, SE France. *Glob. Planet. Change* 92–93, 92–104. doi:10.1016/j.gloplacha.2012.04.007
- Kump, L. R., and Arthur, M. A. (1999). Interpreting carbon-isotope excursions: Carbonates and organic matter. *Chem. Geol.* 161, 181–198. doi:10.1016/s0009-2541(99)00086-8
- Laurin, J., Cech, S., Uličný, D., Zdeněk, S., and Svobodová, M. (2014). Astrochronology of the late turonian: Implications for the behavior of the carbon cycle at the demise of peak greenhouse. *Earth Planet. Sci. Lett.* 394, 254–269. doi:10.1016/j.epsl.2014.03.023
- Leandro, C. G., Savian, J. F., Kochhann, M. V. L., Franco, D. R., Coccioni, R., Frontalini, F., et al. (2022). Astronomical tuning of the Aptian stage and its implications for age recalibrations and paleoclimatic events. *Nat. Commun.* 13, 2941. doi:10.1038/s41467-022-30075-3
- Leckie, R. M., Bralower, T. J., and Cashman, R. (2002). Oceanic anoxic events and plankton evolution: Biotic response to tectonic forcing during the mid-Cretaceous. *Paleoceanography* 17, 13–29. doi:10.1029/2001PA000623
- Lenz, K. L., Pils, W., and Uffenorde, H. (1986). *Geowissenschaftliche Vororgeuntersuchungen zur Standortfindung für die Ablagerung von Sonderabfällen: Abschlussbericht - teil 3,2: Geologische Aufnahme Band 3: Kernbeschreibung*. Nieders: Landesamt f. Bodenforschung.
- Lini, A., Weissert, H., and Erba, E. (1992). The Valanginian carbon isotope event - a first Episode of greenhouse climate conditions during the Cretaceous. *Terra nova*. 4, 374–384. doi:10.1111/j.1365-3121.1992.tb00826.x
- Litke, R., Jendrzewski, L., Lokay, P., Wang, S. Q., and Rullkotter, J. (1998). Organic geochemistry and depositional history of the Barremian–Aptian boundary interval in the Lower Saxony Basin, northern Germany. *Cretac. Res.* 19, 581–614. doi:10.1006/cres.1998.0121
- Marshall, J. D. (1992). Climatic and oceanographic isotopic signals from the carbonate rock record and their preservation. *Geol. Mag.* 129, 143–160. doi:10.1017/S0016756800008244
- Martinez, M., Deconinck, J.-F., Pellenard, P., Riquier, L., Company, M., Reboulet, S., et al. (2015). Astrochronology of the Valanginian–Hauterivian stages (early cretaceous): Chronological relationships between the Parana–Etendeka large igneous province and the Weissert and the Faraoni events. *Glob. Planet Change* 131, 158–173. doi:10.1016/j.gloplacha.2015.06.001
- Maslin, M. A., and Swann, G. E. A. (2006). “Isotopes in marine sediments,” in *Isotopes in palaeoenvironmental research developments in paleoenvironmental research*. Editor M. J. Leng (Dordrecht: Kluwer Academic Publishers), 227–290. doi:10.1007/1-4020-2504-1_06
- Matsumoto, H., Coccioni, R., Frontalini, F., Shirai, K., Jovane, L., Trindade, R., et al. (2022). Mid-Cretaceous marine Os isotope evidence for heterogeneous cause of oceanic anoxic events. *Nat. Commun.* 13, 239. doi:10.1038/s41467-021-27817-0
- McAnena, A., Flögel, S., Hofmann, P., Herrle, J. O., Griesand, A., Pross, J., et al. (2013). Atlantic cooling associated with a marine biotic crisis during the mid-Cretaceous period. *Nat. Geosci.* 6, 558–561. doi:10.1038/ngeo1850
- Menegatti, A. P., Weissert, H., Brown, R. S., Tyson, R. V., Farrimond, P., Strasser, A., et al. (1998). High-resolution $\delta^{13}\text{C}$ stratigraphy through the early aptian “livello selli” of the alpine Tethys. *Paleoceanography* 13, 530–545. doi:10.1029/98PA01793
- Meyer, K. M., Yu, M., Lehmann, D., van de Schootbrugge, B., and Payne, J. L. (2013). Constraints on Early Triassic carbon cycle dynamics from paired organic and inorganic carbon isotope records. *Earth Planet. Sci. Lett.* 361, 429–435. doi:10.1016/j.epsl.2012.10.035
- Mitchell, S., Paul, C., and Gale, A. (1996). Carbon isotopes and sequence stratigraphy. *Geol. Soc. Lond. - Special Publ.* 104, 11–24. doi:10.1144/GSL.SP.1996.104.01.02
- Möller, C., Bornemann, A., and Mutterlose, J. (2020). Climate and paleoceanography controlled size variations of calcareous nannofossils during the Valanginian Weissert Event (Early Cretaceous). *Mar. Micropaleontol.* 157, 101875. doi:10.1016/j.marmicro.2020.101875
- Morales, C., Gardin, S., Schnyder, J., Spangenberg, J., Arnaud-Vanneau, A., Arnaud, H., et al. (2013). Berriasian and early valanginian environmental change along a transect from the juria platform to the Vocontian Basin. *Sedimentology* 60, 36–63. doi:10.1111/sed.12019
- Mutterlose, J., and Böckel, B. (1998). The barremian–aptian interval in NW Germany: A review. *Cretac. Res.* 19, 539–568. doi:10.1006/cres.1998.0119
- Mutterlose, J., and Bornemann, A. (2000). Distribution and facies patterns of lower cretaceous sediments in northern Germany: A review. *Cretac. Res.* 21, 733–759. doi:10.1006/cres.2000.0232
- Mutterlose, J., Bornemann, A., Luppold, F. W., Owen, H. G., Ruffell, A., Weiss, W., et al. (2003). The Vöhrum section (northwest Germany) and the Aptian/Albian boundary. *Cretac. Res.* 24, 203–252. doi:10.1016/S0195-6671(03)00043-0
- Mutterlose, J., and Bornemann, A. (2002). “North Germany: the Early Cretaceous gateway between the Tethys and the Boreal Realm,” in *Tethyan/Boreal Cretaceous Correlation Mediterranean and Boreal Cretaceous palaeobiogeographic areas in Central and Eastern Europe*. Editor J. Michalik (Berlin, Germany: Springer), 213–234.
- Mutterlose, J., Pauly, S., and Steuber, T. (2009). Temperature controlled deposition of early Cretaceous (Barremian–early Aptian) black shales in an epicontinental sea. *Paleoogeogr. Palaeoclimatol. Palaeoecol.* 273, 330–345. doi:10.1016/j.palaeo.2008.04.026
- Nebe, D. W. (1999). *Zyklusuntersuchungen an unterkretazischen Sedimenten in NW-Deutschland - Nachweisbarkeit von Milankovitch-Zyklen*. Phd thesis. Ruhr-Univ. Bochum.
- Ogg, J. G. (2020). Geomagnetic polarity time scale. *Geol. Time Scale* 2020, 159–192. doi:10.1016/B978-0-12-824360-2.00005-X
- Owen, H. G. (2007). Ammonite biostratigraphy of the albian in the Kirchrode II borehole, hannover, Germany. *Cretac. Res.* 28, 921–938. doi:10.1016/j.cretres.2007.01.003
- Papadomanolaki, N. M., van Helmond, N. A. G. M., Pälike, H., Sluijs, A., and Slomp, C. P. (2022). Quantifying volcanism and organic carbon burial across Oceanic Anoxic Event 2. *Geology* 50, 511–515. doi:10.1130/g49649.1
- Paul, C., Mitchell, S., Marshall, J., Leafy, P., Gale, A., Duane, A., et al. (1994). Palaeoceanographic events in the middle cenomanian of northwest Europe. *Cretac. Res.* 15, 707–738. doi:10.1006/cres.1994.1039
- Pauly, D., and Mutterlose, S. J. (2013). Palaeoceanography of Lower Cretaceous (Barremian–Lower Aptian) black shales from northwest Germany evidenced by calcareous nannofossils and geochemistry. *Cretac. Res.* 42, 28–43. doi:10.1016/j.cretres.2013.01.001
- Percival, L. M. E., Tedeschi, L. R., Creaser, R. A., Bottini, C., Erba, E., Giraud, F., et al. (2021). Determining the style and provenance of magmatic activity during the early aptian oceanic anoxic event (OAE 1a). *Glob. Planet. Change* 200, 103461. doi:10.1016/j.gloplacha.2021.103461
- Polteau, S., Hendriks, B. W. H., Planke, S., Ganerød, M., Corfu, F., Faleide, J. I., et al. (2016). The early cretaceous barents sea sill complex: Distribution, $^{40}\text{Ar}/^{39}\text{Ar}$ geochronology, and implications for carbon gas formation. *Paleoogeogr. Palaeoclimatol. Palaeoecol.* 441, 83–95. doi:10.1016/j.palaeo.2015.07.007
- Reichert, K. (2005). *Late aptian-albian of the Vocontian Basin (SE-France) and albian of NE-Texas: Biostratigraphic and paleoceanographic implications by planktic foraminifera faunas*. Phd thesis. University of Tübingen.
- Renard, M. (1986). Pelagic carbonate chemostratigraphy (Sr, Mg, 18O, 13C). *Mar. Micropaleontol.* 10, 117–164. doi:10.1016/0377-8398(86)90027-7
- Rückheim, S., Bornemann, A., and Mutterlose, J. (2006). Integrated stratigraphy of an early cretaceous (Barremian–Early albian) North Sea borehole (BGS 81/40). *Cretac. Res.* 27, 447–463. doi:10.1016/j.cretres.2005.07.005
- Saltzman, M. R., and Thomas, E. (2012). Carbon isotope stratigraphy. *Geol. Time Scale* 2012, 207–232. doi:10.1016/B978-0-444-59425-9.00011-1

- Schlanger, S. O., Arthur, M. A., Jenkyns, H. C., and Scholle, P. A. (1987). The Cenomanian-Turonian Oceanic Anoxic Event, I. Stratigraphy and distribution of organic carbon-rich beds and the marine $\delta^{13}\text{C}$ excursion. *Mar. Pet. source rocks* 26, 371–399. doi:10.1144/gsl.sp.1987.026.01.24
- Scholle, P. A., and Arthur, M. A. (1980). Carbon isotope fluctuations in Cretaceous pelagic limestones: Potential stratigraphic and petroleum exploration tool. *AAPG Bull.* 64, 67–87.
- Selby, D., Mutterlose, J., and Condon, D. J. (2009). U–Pb and Re–Os geochronology of the Aptian/Albian and Cenomanian/Turonian stage boundaries: Implications for timescale calibration, osmium isotope seawater composition and Re–Os systematics in organic-rich sediments. *Chem. Geol.* 265, 394–409. doi:10.1016/j.chemgeo.2009.05.005
- Sprovieri, M., Cocconi, R., Lirer, F., Pelosi, N., and Lozar, F. (2006). Orbital tuning of a lower Cretaceous composite record (Maiolica Formation, central Italy). *Paleoceanography* 21, 1224. doi:10.1029/2005PA001224
- Swart, P. K., and Eberli, G. (2005). The nature of the $\delta^{13}\text{C}$ of periplatform sediments: Implications for stratigraphy and the global carbon cycle. *Sediment. Geol.* 175, 115–129. doi:10.1016/j.sedgeo.2004.12.029
- Thöle, H., Bornemann, A., Heimhofer, U., Luppold, F. W., Blumenberg, M., Dohrmann, R., et al. (2020). Using high-resolution XRF analyses as a sequence stratigraphic tool in a mudstone-dominated succession (Early Cretaceous, Lower Saxony Basin, Northern Germany). *Depositional Rec.* 6, 236–258. doi:10.1002/dep2.83
- Thöle, H. (2017). *Research project sequenzstratigraphie tiefere Unterkreide TUNB. - final and interim reports.* Germany: Unpublished report – BGR.
- Turgeon, S. C., and Creaser, R. A. (2008). Cretaceous Oceanic Anoxic Event 2 triggered by a massive magmatic episode. *Nature* 454, 323–326. doi:10.1038/nature07076
- Tyson, R. V. (1995). *Sedimentary organic matter - organic facies and palynofacies.* Dordrecht: Springer. doi:10.1007/978-94-011-0739-6
- van de Schootbrugge, B., Föllmi, K. B., Bulot, L. G., and Burns, S. J. (2000). Paleoenvironmental changes during the Early Cretaceous (Valanginian-Hauterivian): Evidence from oxygen and carbon stable isotopes. *Earth Planet. Sci. Lett.* 181, 15–31. doi:10.1016/S0012-821X(00)00194-1
- Voigt, S., Erbacher, J., Mutterlose, J., Weiss, W., Westerhold, T., Wiese, F., et al. (2008). The Cenomanian–Turonian of the Wunstorf section (north Germany): Global stratigraphic reference section and new orbital time scale for oceanic anoxic event 2. *Newsletters Stratigr.* 43, 65–89. doi:10.1127/0078-0421/2008/0043-0065
- Voigt, S., and Hilbrecht, H. (1997). Late Cretaceous carbon isotope stratigraphy in Europe: Correlation and relations with sea level and sediment stability. *Palaeoogeogr. Palaeoecol.* 134, 39–59. doi:10.1016/S0031-0182(96)00156-3
- Voigt, S., Püttmann, T., Mutterlose, J., Bornemann, A., Jarvis, I., Pearce, M., et al. (2021). Reassessment of the Salzgitter-Salder section as a potential stratotype for the Turonian-Coniacian boundary: Stable carbon isotopes and cyclostratigraphy constrained by calcareous nannofossils and palynology. *Newsletters Stratigr.* 54, 209–228. doi:10.1127/nos/2020/0615
- Voigt, S., and Wagreich, M. (2008). “Cretaceous,” in *Geology of central Europe.* Editor T. McCann (United States: Geological Society Publishing House), 923–997.
- von Strandmann, P. A. E. P., Kasemann, S. A., and Wimpenny, J. B. (2020). Lithium and lithium isotopes in earth's surface cycles. *Elements* 16, 253–258. doi:10.2138/elements.16.4.253
- Walaszczyk, I., Čech, S., Crampton, J. S., Dubicka, Z., Ifrim, C., Jarvis, I., et al. (2021). The global boundary stratotype section and point (GSSP) for the base of the coniacian stage (Salzgitter-Salder, Germany) and its auxiliary sections (ślupia nadbrzeżna, central Poland; střeleč, Czech republic; and el rosario, NE Mexico). *Episodes* 45, 181–220. doi:10.18814/epiugs/2021/021022
- Wefer, G., and Berger, W. H. (1991). Isotope paleontology - growth and composition of extant calcareous species. *Mar. Geol.* 100, 207–248. doi:10.1016/0025-3227(91)90234-U
- Weissert, H., and Erba, E. (2004). Volcanism, CO₂ and palaeoclimate: A late Jurassic–Early Cretaceous carbon and oxygen isotope record. *J. Geol. Soc.* 161, 695–702. doi:10.1144/0016-764903-087
- Weissert, H. J. (1979). *Die Paläoozeanographie der südwestlichen Tethys in der Unterkreide.* Berlin: Springer.
- Weissert, H., Joachimski, M., and Sarnthein, M. (2008). Chemostratigraphy. *Newsletters Stratigr.* 42, 145–179. doi:10.1127/0078-0421/2008/0042-0145
- Weissert, H., Lini, A., Föllmi, K. B., and Kuhn, O. (1998). Correlation of early cretaceous carbon isotope stratigraphy and platform drowning events: A possible link? *Palaeoogeogr. Palaeoecol.* 137, 189–203. doi:10.1016/S0031-0182(97)00109-0
- Wendler, I. (2013). A critical evaluation of carbon isotope stratigraphy and biostratigraphic implications for Late Cretaceous global correlation. *Earth Sci. Rev.* 126, 116–146. doi:10.1016/j.earscirev.2013.08.003
- Westerhold, T., Marwan, N., Drury, A. J., Liebrand, D., Agnini, C., Anagnostou, E., et al. (2020). An astronomically dated record of Earth's climate and its predictability over the last 66 million years. *Science* 369, 1383–1387. doi:10.1126/science.aba6853
- Wilmsen, M. (2007). Integrated stratigraphy of the upper lower-lower Middle Cenomanian of northern Germany and southern England. *Acta Geol. Pol.* 57, 263–279.
- Wilson, P. A., and Norris, R. D. (2001). Warm tropical ocean surface and global anoxia during the mid-Cretaceous period. *Nature* 412, 425–429. doi:10.1038/35086553
- Wortmann, U. G., and Weissert, H. (2000). Tying platform drowning to perturbations of the global carbon cycle with a $\delta^{13}\text{C}_{\text{org}}$ -curve from the Valanginian of DSDP Site 416. *Terra nova.* 12, 289–294. doi:10.1046/j.1365-3121.2000.00312.x
- Wulff, L., Mutterlose, J., and Bornemann, A. (2020). Size variations and abundance patterns of calcareous nannofossils in mid Barremian black shales of the Boreal Realm (Lower Saxony Basin). *Mar. Micropaleontol.* 156, 101853. doi:10.1016/j.marmicro.2020.101853
- Zheng, X.-Y., Jenkyns, H. C., Gale, A. S., Ward, D. J., and Henderson, G. M. (2016). A climatic control on reorganization of ocean circulation during the mid-Cenomanian Event and Cenomanian-Turonian oceanic anoxic event (OAE 2): Nd isotope evidence. *Geology* 44, 151–154. doi:10.1130/G37354.1